Bias and Bias Line Effects on Wideband RF Power Amplifier Performance

William Sear, Devon T. Donahue, Michelle Pirrone, and Taylor W. Barton

RF Power and Analog Laboratory

Department of Electrical, Computer, and Energy Engineering, University of Colorado Boulder

william.sear@colorado.edu, taylor.w.barton@colorado.edu

Abstract—The challenges associated with efficiently and effectively linearizing a nonlinear power amplifier (PA) over wide signal bandwidths are increasingly important to the design of 5G front-ends. Conventional digital linearization techniques are limited by absolute bandwidth, while the RF-domain nonlinear PA typically exhibits consistent fractional bandwidth even as the carrier frequency is increased. Therefore, RF-domain design techniques, like those focusing on bias-line impedance selection, are critical for overall distortion reduction. To evaluate bias-line effects, a demonstrator PA is here investigated over a range of Class-AB biases and over a range of drain inductance values. The characterization under two-tone and LTE-like modulated excitations with 10-MHz and 100-MHz instantaneous bandwidth shows that the conventional linear-efficiency trade-off in bias design does not necessarily hold true for wide instantaneous bandwidths. Additionally, techniques to synthesize a negative baseband impedance using low frequency feedback are discussed.

I. INTRODUCTION

Emerging wireless systems increasingly require RF and millimeter-wave (mm-wave) front-ends with high instantaneous bandwidths to support demands for high data rates. Whereas previous generations of hardware could rely on relatively narrowband impedance matching and bias structures, scaling these to wide bandwidths is not straightforward. Similarly, linearization techniques — conventionally performed in the digital domain — face scaling challenges when the absolute bandwidth increases. Significant research effort has been directed towards increasing RF bandwidth in power amplifiers (PAs) [1], [2], but high instantaneous bandwidth (IBW) cannot be assumed to automatically follow due to the need to oversample the RF signal in the digital domain [3].A transmitter block diagram illustrating the tradeoffs assocaited with the fractional bandwidth scaling present in RF analog devices and the absolute bandwidth scaling present in digital systems is shown in Fig. 1. The challenges associated with moving to higher instantaneous bandwidth signals have encouraged the adoption of various hybrid analog and digital linearization methods that take advantage of analog frequency scaling effects to augment existing digital methods [4], [5].

To support to these system level changes, the PA designer can take simple steps to improve the linearizability and baseline distortion introduced by the PA. In particular, the biasing

This material is based on work supported by the National Science Foundation under Grant No. 1846507.

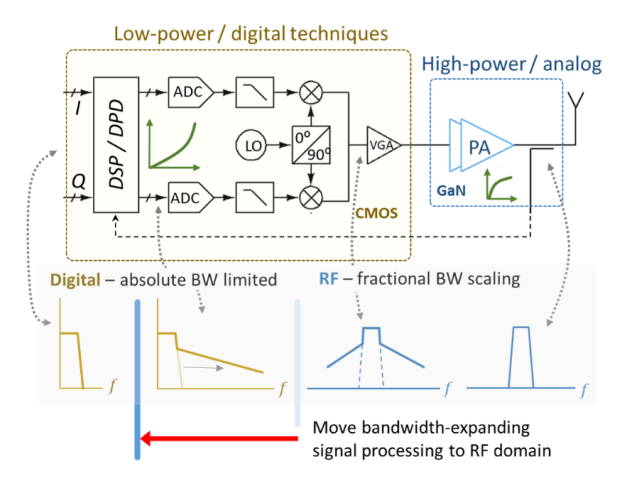


Fig. 1: Transmitter block diagram illustrating bandwidth expansion effects from digital pre-distortion. Performing signal processing in the RF domain exploits fractional bandwidth scaling, critical for wide instantaneous bandwidth signals.

structure used in a design can dramatically alter the distortion generated in a PA, most noticeably if it presents an impedance that varies significantly over the modulation frequencies [6], [7]. In this work, we consider the observed performance of a PA under differing gate bias points and baseband impedances to showcase the sometimes unexpected performance differences between CW and two-tone tests compared to real wideband modulated signals. Using low frequency feedback to synthesize more desirable baseband impedances will also be discussed.

II. HIGH IBW SIGNAL DISTORTION CHARACTERISTICS

While distortion in weakly nonlinear PAs is well described mathematically for simple excitations such as two-tone signals, most analysis makes a narrowband assumption [8] that loses validity in modern communication systems where instantaneous bandwidths commonly approach or exceed 100-MHz of the carrier frequency. As a result, comparing two PAs based on IMD3 response to two-tone excitation does not meaningfully translate to real signals [9]. Similarly, PA efficiency has been observed to degrade for wideband signals beyond the expected performance extrapolated from CW characterization [10].

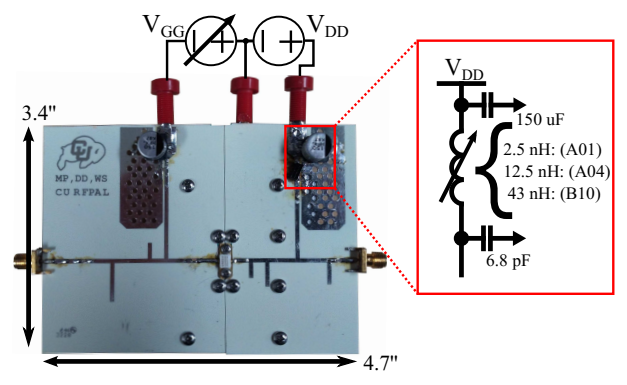


Fig. 2: Photograph of the PA used to evaluate performance as bias condition and drain inductor are varied.

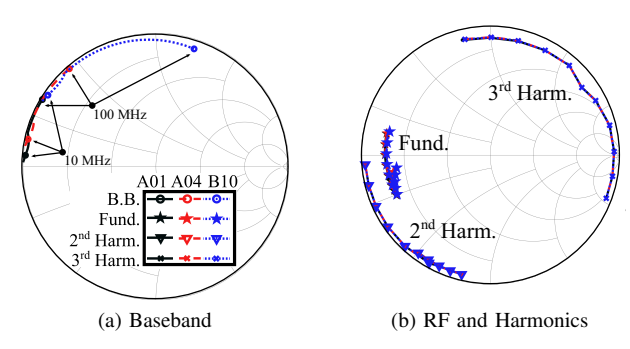


Fig. 3: Simulated drain impedances presented to the transistor at (a) baseband (dc, 10-MHz, and 100-MHz) and (b) the fundamental (1.9-2.4 GHz) and the $2^{\rm nd}$ and $3^{\rm rd}$ harmonics.

To demonstrate these effects, a PA based on the Wolfspeed CG2H40010 GaN device operating at 2.15 GHz was designed in which the gate bias point and baseband impedance terminating the drain can be varied to compare performance. As shown in Fig. 2, the output matching network is connected to the drain supply through a $\lambda/4$ line at 2.15 GHz that is terminated by a 6.8-pF capacitor. Between the 6.8-pF capacitor and a 150-uF baseband capacitor one of three candidate inductors is soldered in place to fix the baseband drain impedance without perturbing the fundamental and harmonic impedances. We use inductors from the Coilcraft Mini Aircore AxxT/BxxT product line [11] which are here referenced using the first three digits of their Coilcraft part number.

The simulated impedances presented to the package plane for inductor values of 2.5-nH (A01), 12.5-nH (A04), and 43-nH (B10), shown in Fig. 3, are nearly constant at the RF carrier frequency and harmonics despite the different Q factors, resonant frequencies, and dc resistances of each inductor, while the baseband impedances vary depending on the inductor as expected. The fundamental and harmonic terminations are selected based on load-pull simulation at a 150-mA quiescent current corresponding to class-AB operation with a flat transconductance response to minimize sensitivity to gate bias point.

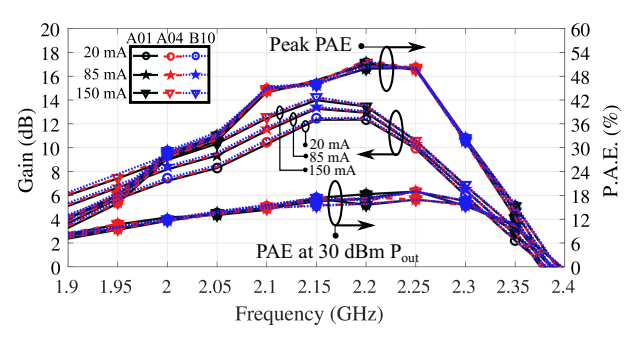


Fig. 4: Measured CW results for gain and PAE at 30 dBm output power and peak PAE from 1.9 GHz to 2.4 GHz.

In this study, we evaluate the PA's performance under twotone and LTE signal excitation to compare how the selection of gate bias point and drain inductor affect the linearity. We expect that higher inductor values will cause greater selfmodulation effects, introducing distortion products. Similarly, a straightforward tradeoff in efficiency and linearity through bias point selection is anticipated.

The PA is first characterized under CW excitation across frequency as shown in Fig. 4, which plots both peak PAE and the PAE for a fixed 30-dBm output power corresponding to approximately 10-dB output power back-off. For this and all following measurements, the PA is measured with all nine possible combinations of the three bias conditions and three inductor values in the drain supply network. Across the measured 500 MHz range, the PAE at 30-dBm output power and maximum PAE values are consistent, staying within 3 percentage points of each other. The gain of the PA across the band is independent of inductor selection, but higher bias currents result in higher gains with the 150-mA bias having 2-dB higher gain than the 20-mA bias. The measured gain and efficiency response is reasonably consistent over the 100-MHz maximum instantaneous bandwidth of the LTE test signals that will be evaluated later in this section.

Fig. 5 presents the measured average third order intermodulation distortion products (IMD3) and PAE under each bias and inductor test condition for two-tone tests without digital predistortion (DPD). Fig. 5(a) presents the response of a 10-MHz two-tone test which shows a "sweet-spot" [12] behavior around 34-dBm as a function of bias condition but little dependence on baseband condition. In contrast, the 100-MHz twotone IMD3 response [Fig. 5(b)] exhibits a greater dependence on baseband impedance. Above 25-dBm output power the IMD3 response is primarily driven by baseband impedance with smaller baseband impedances resulting in lower IMD3 products. Interestingly in the lowest baseband impedance case (A01 inductor), the lowest IMD3 products above 25-dBm output power are in the 20-mA bias condition, which also has the highest PAE of the tested bias and impedance conditions. This suggests that for wide instantaneous bandwidth signals the conventional linearity-efficiency trade-off in bias design does not necessarily hold true.

To better understand the practical behavior of the linearity-

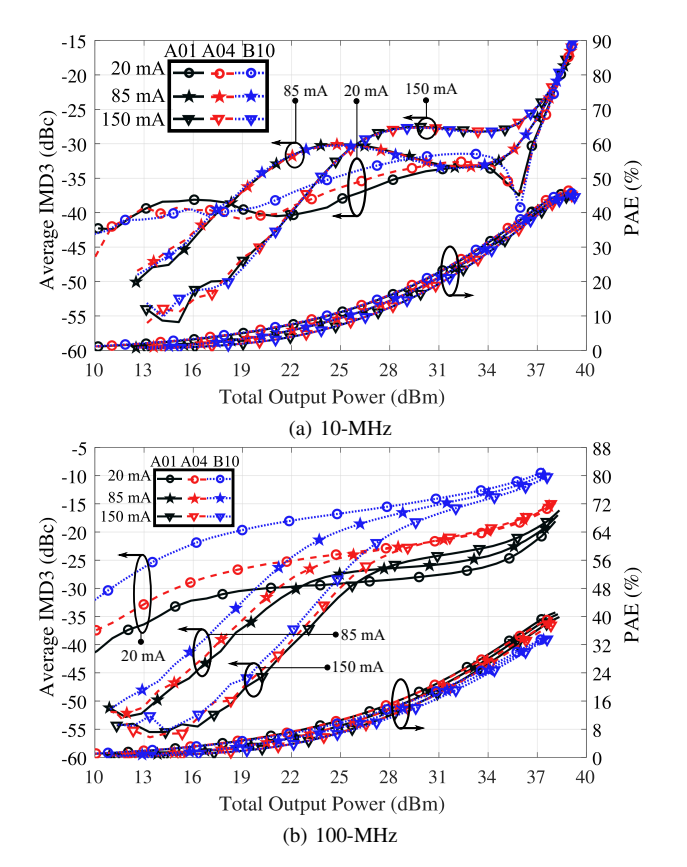


Fig. 5: Measured average IMD3 products and PAE over bias and baseband impedance for a two-tone signal centered at 2.15 GHz with (a) 10-MHz and (b) 100-MHz tone spacing. No DPD techniques have been applied.

efficiency trade-off in a communications system we characterize the PA over bias and impedance with LTE-like signals. The experimental setup is based on a Rohde & Schwarz FSW43 which generates and measures the signals using the K-18 PA measurement application. A blind receiver equalizer was applied but no DPD techniques were applied to any of the measured results.

Fig. 6(a) presents the measured mean error vector magnitude (EVM) and average PAE of a 10-MHz LTE-like signal where all measured output crest factors are 9.6-dB. As in the two-tone case the measured average PAE is only a function of gate bias point selection with the 20-mA bias having highest efficiency and 150-mA bias having lowest efficiency, as expected. In contrast to the two-tone case, in the EVM result there is a greater dependence on baseband impedance than expected. However, the "sweet-spot" behavior seen in the two-tone case for the 85-mA and 20-mA bias conditions also appears in the modulated signal behavior. Most interestingly, the up to 4 percentage point improvement in EVM observed in the 85-mA bias case is predicted neither by the IMD3 results nor by conventional wisdom.

Fig. 6(b) presents the measured mean EVM and average PAE of a 100-MHz LTE-like signal where all measured output crest factors are 9.6-dB. Again the PAE follows the expected

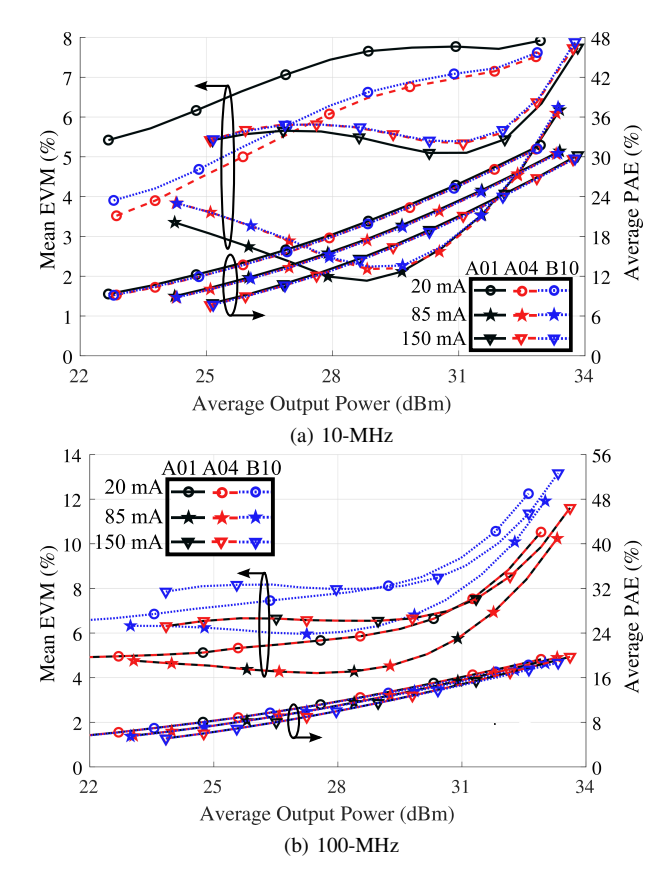


Fig. 6: Measured mean EVM and PAE over bias and baseband impedance for an LTE-like 9.6 dB PAPR signal centered at 2.15 GHz with bandwidths of (a) 10-MHz and (b) 100-MHz. An equalizer was applied in the receiver, but no DPD techniques have been applied.

trend with bias condition and is largely independent of the baseband impedance. In contrast to the 10-MHz LTE-like signal but as in the 100-MHz two-tone IMD3 no "sweet-spot" behavior appears in the mean EVM. The optimum condition for combined EVM and PAE metrics is the 85-mA bias condition with either the A01 or A04 inductor, similar to what is observed with the 10-MHz LTE-like signal. The optimality of the 85-mA bias condition is as prominent in this 100-MHz signal compared to the 10-MHz signal, but the difference in average PAE associated with gate bias point selection is less significant, with at most 1 percentage point difference. Across all bias conditions the effect of the inductor selection is also more prominent in the mean EVM, with the B10 inductor showing between 1 and 2 percentage point increases in EVM compared to the A01 or A04 inductors. In both the 10-MHz and 100-MHz signals the measured ACPR follows the same trends over average power as the mean EVM.

III. ACTIVE CONTROL OF BASEBAND IMPEDANCES

While selection of optimal baseband impedances can improve the performance of a PA in a practical system, the designer is fundamentally limited by the quality of the components available to them. This issue can be resolved, and

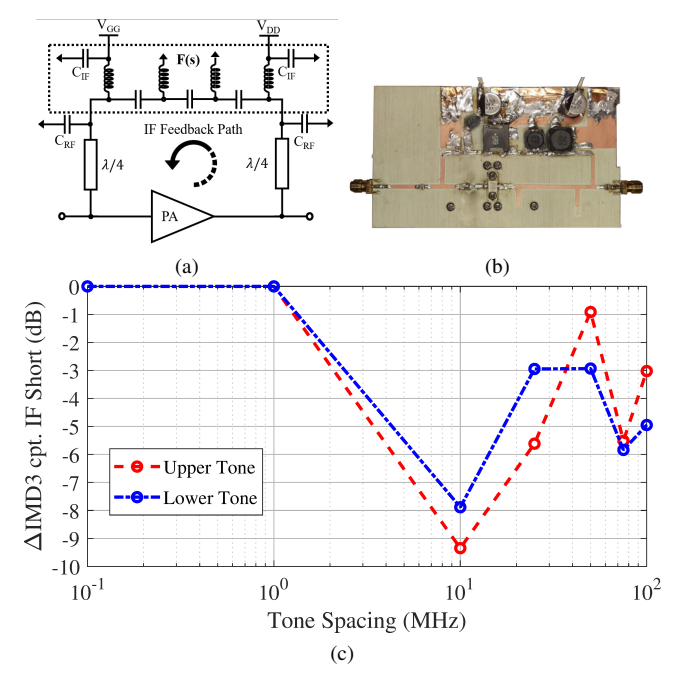


Fig. 7: IF Feedback amplifier (a) Block diagram of amplifier with 7-pole feedback network, (b) photograph of the fabricated amplifier, and (c) measured IMD3 difference in feedback compared to a shorted-baseband termination at 42.5 dBm output power (P3dB) measured across two-tone spacing. [14]

the IMD3 improved even beyond an ideal passive baseband termination, by synthesizing a negative baseband-frequency or intermediate-frequency (IF) impedance at the drain of the device [13]. This can be accomplished by feeding the baseband tones generated at the transistor drain back to the gate, so that they are amplified by the low-frequency gain of the device. The behavior of the negative IF impedance can then be easily controlled through the selection of the feedback network, which is most conveniently implemented as an LC ladder network which, when implemented shunt element first, provides a biasing inductor and a dc blocking capacitor for both the gate and drain as shown in Fig. 7(a). A network that synthesizes a negative impedance between 1 and 100 MHz designed for a 15 W PA operating at 2.14 GHz was implemented as shown in Fig. 7(b). The measured design demonstrates IMD3 suppression of both tones over 1-MHz to 100-MHz range at the 41.5 dBm output power as can be seen in Fig. 7(c), with maximum suppression occurring at 10 MHz. This technique presents a promising option for enabling wider instantaneous bandwidth signals at arbitrary power levels. Additional details regarding this PA and network design can be found in [14].

IV. CONCLUSION

In this work the effect of gate bias point selection and baseband impedance presented to the drain of a PA is investigated. When conventional passive termination is employed, the measured linearity-efficiency tradeoff under two-tone excitation largely follows the expected behavior, although with perhaps less dependence on baseband impedance than expected. On the other hand, the results with LTE-like signals demonstrate that selecting a higher quiescent current bias does not necessarily improve the linearity of the PA, contrary to the predicted behavior based on IMD measurement. These results suggest that bias and bias line effects are best selected based on characterization with real signals to be used in the intended PA application.

Active baseband impedance control techniques, although a relatively new and unexplored technique, can potentially further improve linearity by producing negative baseband terminating impedances. Preliminary results with two-tone signals demonstrate the technique can simultaneously suppress both upper and lower IMD3 tones, and over a wide range of tone spacing without perturbing the baseline RF performance of the PA. Both approaches for controlling baseband impedances can scale to higher carrier frequencies where the wider absolute instantaneous bandwidths pose a challenge for DPD.

REFERENCES

- S. Bayaskar, P. de Falco, and T. Barton, "A 2.4/3.5 GHz dual-band power amplifier with filter-based bias network and SRFT matching," in *European Microw. Conf.*, 2021, pp. 5–8.
- [2] A. Bogusz, Z. Costello, R. Quaglia, J. Bell, et al., "Power and efficiency continuous modes in saturated GaN HEMT devices," in Intl. Workshop on Integrated Nonlinear Microwave and Millimetre-wave Circuits (IN-MMIC), 2018, pp. 1–3.
- [3] C. Yu, D. Hou, H. Sun, F. Meng, et al., "A reconfigurable in-band digital predistortion technique for mmWave power amplifiers excited by a signal with 640 MHz modulation bandwidth," in European Microw. Integrated Circuits Conf., 2017, pp. 306–309.
- [4] P.M. Tomé, F.M. Barradas, T.R. Cunha, and J.C. Pedro, "Hybrid analog/digital linearization of GaN HEMT-based power amplifiers," *IEEE Trans. Microw. Theory Techn.*, vol. 67, no. 1, pp. 288–294, 2019.
- [5] R.N. Braithwaite, "Using a cascade of digital and analog predistortion to linearize a dual-band rf transmitter," in *IEEE Topical Conference on RF/Microwave Power Amplifiers for Radio and Wireless Applications* (PAWR), 2017, pp. 77–80.
- [6] B. Bunz, A. Ahmed, and G. Kompa, "Influence of envelope impedance termination on RF behaviour of GaN HEMT power devices," in European Gallium Arsenide and Other Semiconductor Application Symp., 2005, pp. 649–652.
- [7] D.R. Barros, L.C. Nunes, P.M. Cabral, and J.C. Pedro, "Impact of the input baseband terminations on the efficiency of wideband power amplifiers under concurrent band operation," *IEEE Trans. Microw. Theory Techn.*, vol. 67, no. 12, pp. 5127–5138, 2019.
- [8] S.C. Cripps, RF Power Amplifiers for Wireless Communication. Norwood, MA: Artech House, 2006.
- [9] W. Hallberg, P.E. de Falco, M. Özen, C. Fager, et al., "Characterization of linear power amplifiers for LTE applications," in *IEEE Topical* Conference on RF/Microwave Power Amplifiers for Radio and Wireless Applications, 2018, pp. 32–34.
- [10] L.C. Nunes, D.R. Barros, P.M. Cabral, and J.C. Pedro, "Efficiency degradation analysis in wideband power amplifiers," *IEEE Trans. Microw. Theory Techn.*, vol. 66, no. 12, pp. 5640–5651, 2018.
- [11] "Mini air core inductors," Coilcraft, Tech. Rep. 107-1, October 2011.
- [12] P.E. de Falco, J. Birchall, and L. Smith, "Hitting the sweet spot: A single-ended power amplifier exploiting class AB sweet spots and optimized third harmonic termination," *IEEE Microw. Mag.*, vol. 18, no. 1, pp. 63–70, 2017.
- [13] M. Akmal, J. Lees, S. Bensmida, S. Woodington, et al., "The effect of baseband impedance termination on the linearity of GaN HEMTs," in European Microw. Conf., 2010, pp. 1046–1049.
- [14] W. Sear and T.W. Barton, "Wideband IMD3 suppression through negative baseband impedance synthesis," *IET Microwaves, Antennas & Propagation*, vol. 15, no. 7, pp. 728–743.